Hybridization strength in Ce compounds: A local-density study

Lukas Severin* and Börje Johansson
Condensed Matter Theory Group, Department of Physics, University of Uppsala, Box 530, S-75121 Uppsala, Sweden
(Received 13 May 1994)

A systematic *ab initio* electronic-structure study of the late transition-metal–cerium compounds forming in the cubic Laves-phase structure, and of those cerium compounds ($CeRh_3$, $CePd_3$, and $CePt_3$) forming in the $AuCu_3$ structure, is performed using the local-density approximation. Magnetic and cohesive properties are shown to be crucially dependent on the treatment of the cerium $4f$ electron. In all cases investigated (except for the palladium and platinum compounds) our calculations favor a picture with delocalized $4f$ electrons. Photoemission data for the strongly $4f$-$4d$ hybridized $CeRh_3$ system is discussed and shown to have a substantial itinerant $4f$ character. Calculations for some fictitious $AuCu_3$ compounds CeA_3, where A is a $4d$ element preceding Rh or a $5d$ element preceding Pt, are also presented. This is done in order to elucidate how the position of the cerium $4f$ band, relative to the Fermi level, changes when such a series of compounds is traversed. The hybridization between the cerium $4f$ states and the transition-metal d states is shown to vary in a systematic way, which, together with the filling of the transition-metal d band, can explain the position of the $4f$ band. The calculated $4f$ position is compared with data from inverse photoemission spectroscopy. Especially the anomalous position of the $4f^1$ peak, previously found in bremsstrahlung isochromat spectroscopy experiments for $CeRh_3$, is found to fit into the calculated trend in a consistent manner.

I. INTRODUCTION

Ce metal is probably the most fascinating metallic element in the Periodic Table showing an extraordinarily rich phase diagram.[1] As a function of atomic number, Ce is the first elemental metal with an occupied $4f$ orbital. Due to the relatively extended nature of the $4f$ wave function, when compared with the heavier rare earths, it is generally believed that an appropriate description of the interaction between the $4f$ states and the extended conduction electron states is the key to the understanding of the physics of Ce metal and cerium-based compounds. Most studies[2–4] have been concerned with the isostructural (fcc-fcc) α-γ phase transition accompanied by a huge volume change ($\approx 14\%$). Johansson[3] proposed a model where the α-γ transition was considered as a delocalization of the $4f$ electron in the sea of the other conduction electrons, i.e., a Mott transition within the $4f$ manifold. The large volume collapse is then considered to be due to the bonding contribution from the $4f$ electrons forming a narrow band on the high-pressure (low-volume) side of the transition. In such an approach one might expect a mean-field treatment typical of modern density-functional approaches to give a sufficiently accurate picture.

The opposite starting point is the strong correlation limit and the single impurity (SI) (Refs. 5 and 6) model. Here $4f$ charge fluctuations on each cerium site are strongly suppressed due to large Hubbard-like correlations and the hybridization strength between the $4f$ states and the conduction electrons is represented by an energy-dependent mixing $V(\varepsilon)$. Thus in this model no possibility is taken into account for direct $4f$-$4f$ hopping. This model is mapped onto the Kondo Hamiltonian (through a Schrieffer-Wolff[7] transformation). The physics is now governed by the Kondo temperature T_K and the volume collapse[4] can be described by a volume-dependent Kondo coupling constant. The SI model neglects the interaction between the neighboring impurities. Therefore, if these interactions cannot be neglected a band description of the cerium $4f$ electron may become more appropriate.[8]

Concerning crystallographic phase diagrams for the elemental metals, there exists much confidence in the accuracy of first-principle calculations. Skriver[9] was able to account for the correct crystal structures of the transition metals by a local-density treatment of the contribution to the cohesion from the d electrons as well as from the other valence electrons. Moreover, for cerium, he stressed the importance of the $4f$ electrons and their significance for crystal structure stabilities as a function of pressure. However, his results did not quite reproduce the experimental data. This was later shown, by Eriksson and coworkers,[10] to be due to the shape approximations used by Skriver for the crystal potential, and by using an all electron, full potential and fully relativistic linear muffin-tin orbital (LMTO) method they were able to correctly account for the high-pressure α-α' transition observed experimentally at a pressure of about 65 kbar. With increasing pressure an fcc→orthorombic→bct structure sequence is experimentally observed.[11] Also this could be accounted for by theoretical calculations by Eriksson and co-workers.[10] In these calculations the $4f$ electrons were allowed to be part of the valence-band structure and were thus treated as itinerant. Moreover, Eriksson and coworkers showed (by putting the relevant transfer integrals to zero) that both direct $4f$-$4f$ hopping and $4f$-$5d$ hybridization contributed almost equally to the bandwidth and that these contributions were not additive but strongly $\mathbf{k}$-point dependent. If the direct hopping was

neglected, they obtained an equilibrium volume close to that of γ-cerium. One must, therefore, conclude that there is a very strong evidence for the correctness of itinerant f electron theory for describing the pressure-dependent crystallographic data for cerium metal at $T=0$. More recently, self-interaction corrected (SIC), local-density approximation (LDA) calculations,[12] have been performed on Ce metal. Such calculations give a better treatment of the static part of the $4f$ Coulomb interaction and also have the virtue of being able to distinguish between localized and itinerant electron states. These calculations gave more substantial support to a picture with a localized $4f$ electron in γ-cerium but itinerant in α-cerium.

In cerium intermetallic compounds the direct $4f$-$4f$ overlap is often almost negligible, but the hybridization strength between the $4f$ state and, for example, the d states for a transition-metal partner is often much larger than the corresponding hybridization in Ce metal. It is interesting here to make a comparison with uranium metal and its intermetallic compounds. While it is well known that the $5f$ electrons form band states in uranium metal, in some uranium intermetallics the $5f$ states seem to be more localized than in the corresponding Ce compound. An example of this is UPd_3 and $CePd_3$. The former is a local-moment system[13] whereas the latter is a mixed-valence compound.[14] For cerium and uranium compounds it is thus not clear, *a priori,* whether a band description of the f states is sufficient or if more elaborate models are needed to give a proper description of their electronic structure.[15] As discussed above there is now a general confidence in the predictions of electronic-structure calculations based on the LDA to density-functional theory (DFT) also for systems with quite strongly correlated electrons concerning cohesive properties, crystal structure stabilities as a function of pressure, etc. Even the Fermi surface of the heavy electron material UPt_3 is well accounted for by LDA.[16] A good description of the zero-temperature phase diagram of cerium metal was achieved by treating the $4f$ electrons on the same footing as the other valence electrons, i.e., allowing them to form band states. However, also for cerium compounds a growing number of properties are remarkably well predicted by LDA. As will be discussed below, the magnetism of $CeFe_2$ is well described. Actually, in this system the magnetic moment on the cerium atom is antiparallel to that of the moment on the iron atom because the $4f$ orbital moment is almost quenched due to band formation.[17] A technique for orbital polarization, which makes consistent *ab initio* calculations of both spin and orbital magnetic moments possible, is presented in a forthcoming paper,[18] and there we will discuss the case of $CeFe_2$ in more detail. Also, the magnetic properties of $CeCo_5$ are well reproduced[19] by LDA theory. Magnetic susceptibility enhancements, e.g., in the $CeNi_x$ ($x=1,2,5$) (Refs. 20 and 21) system of compounds, can often be accounted for. The great advantage of a description based on self-consistent band calculations is that they can reveal *trends* in the above mentioned properties in a simple and consistent manner.

On the other hand, mass enhancement, and its contribution to the specific heat, depends on the quasiparticle spectrum of the system considered, and as such is not a ground-state property and must be considered as outside the domain of validity of DFT.[22] Moreover, a band description is clearly unable to account for multiplet effects and satellite features as revealed, e.g., by high-energy spectroscopies.[23] Here, then, the confidence lies in model calculations often based on the impurity model as discussed above. However, also *ab initio* theory[24] can be used in supercell calculations to account for such final-state effects. Thus we have two quite contradictory models that successfully predict different properties of the same systems. It is only natural then to test the limits of applicability of LDA as far as possible.

When probing a system with photoelectron (PE) spectroscopy it is important to have in mind that this technique, to a large extent, probes the surface layers. On the surface the reduced coordination number suggests that the states are more localized than in the interior of the material. This would naturally be more important for those electrons, which, already in the bulk, are on the border to localization. This sensitivity of PE spectroscopy to the surface decreases with increasing energy (beyond a relatively low energy for which there is a maximal surface sensitivity). Thus by analyzing the energy dependence of the PE spectra it has become possible to separate the bulk and surface contributions.[25] Moreover, by appropriate subtraction of so-called off resonance spectra it is also possible to separate out the bulk $4f$ signal with quite high resolution (approximately 40 meV). This has called for a reinterpretation of the model parameters used in the SI model, leading to increased hybridization parameters (Δ), decreased correlation parameters (U) and a decrease of the distance between the $4f$ level and the Fermi energy. This has also led to an increased difficulty in explaining PE and inverse photoemission with the same set of parameters. Naturally x-ray PE and valence-band PE spectroscopy are quite violent processes, the creation of a core hole necessarily contracts the $4f$ orbital and thereby leads to a more localized description of the $4f$ manifold. In inverse photoemission spectroscopy, on the other hand, an electron added to the $4f$ level leads to a more expanded $4f$ orbital and, therefore, to a more delocalized character of the $4f$ states.

The position of the $4f^1$ peak in bremsstrahlung isochromat spectroscopy (BIS) is a physical quantity that depends sensitively on the hybridization strength between the valence states and the $4f$ electron. Naturally, it also depends on the degree of filling of the valence bands, i.e., the position of the Fermi level. Such properties are often well described by first-principle calculations. In Table I we present a collection of experimental data[26] for the distance from the Fermi level to this peak for a number of intermetallic cerium compounds. Except for $CeRh_3$ the position of the $4f^1$ peak lies roughly in the region between 0.4–0.7 eV with an error of approximately 0.2 eV for each compound. Irrespective of the accuracy of these numbers the value for $CeRh_3$ stands out as anomalous. The peak position here is approximately 1.4 eV, higher than in any cerium compound studied so far. $CeRh_3$ is commonly accepted as the most delocalized cerium com-

TABLE I. Position of the $4f^1$ peak (in eV) from inverse photoemission for Ce transition-metal compounds. All the data are estimated from Ref. 26, except $CeRh_3$ which is taken from Ref. 41.

$CePd_3$	0.5
$CePt_3$	0.6
$CeRh_3$	1.4
$CeRu_2$	0.9
$CeCo_2$	0.5
$CeNi_2$	0.5
$CeCo_5$	0.7

pound and naturally sets the limits of the applicability of the impurity model. Also from the data in Table I no absolute trend in these values can be inferred, and it is difficult to understand the unique position among the cerium compounds held by $CeRh_3$.[27] From our point of view it is then a natural test case for LDA, not only in order to account for the position of this peak, which should in principle be possible, but also to put this compound in a wider context, among the other cerium systems. We have performed self-consistent *ab initio* calculations for a large class of cerium compounds with different concentrations and types of ligand atoms. These ligands are all taken from the late part of the *d* transition-metal series.

This paper is organized as follows. In Sec. II we present our LDA calculated results for the Laves-phase compounds CeA_2 (A belongs to the Fe, Co, or Ni group). In Sec. III we present our calculated results for the CeA_3 compounds (A is a $4d$ or $5d$ transition-metal element from the Mn, Fe, Co, or Ni group). As will be seen in Sec. IV, $CeRh_3$ is unique in the sense that the high-energy spectroscopy data cannot be satisfactory explained within the impurity model, whereas a band theoretical treatment might be more appropriate. In Sec. V, $CeRh_3$, and especially the position of its $4f^1$ peak, is shown to be part of a trend in the position of the $4f$ band relative to the ligand d band and as such naturally explains the anomalous behavior of $CeRh_3$. Finally, in Sec. VI we summarize our results.

II. CERIUM LAVES-PHASE COMPOUNDS

In this and the next section we present the results from our calculations. They have been performed using the LMTO method,[28] and for LDA exchange and correlation the von-Barth–Hedin[29] parametrization was used. The cerium compounds CeA_2 (here A denotes a late $3d$, $4d$, or $5d$ transition-metal element) all form in the $A15$ cubic Laves-Phase structure and are thus particularly useful for study. From a theoretical point of view it is then possible to elucidate trends in the properties of the materials as a function of band filling, band position, and hybridization strength.

In Figs. 1–3 we present our calculated paramagnetic density of states (DOS) for these compounds. As can be seen from Fig. 1 the hybridization between the $4f$ states and the $3d$ states decreases as the number of $3d$ electrons increases when going from $CeFe_2$ to $CeNi_2$. For the transition-metal atoms the d level drops in energy as the number of d electrons increases, due to the attractive potential from the added nuclear charge, and since this level corresponds to the center of the d band when transition-metal atoms are brought together to form the elemental metal, the center of the d band drops in energy as well, as the d band gets progressively filled. A consequence of this is that the $3d$ orbitals contract and, therefore, the overlap between the wave function from different sites decreases, leading to a narrowing of the d band. These effects are well known for the simple transition metals, but it would be interesting to study its influence on the cerium atom in an intermetallic compound. In the case of the cerium compounds studied here, the above-mentioned mechanism affects the strength of the hybridization between the transition-metal d states and the cerium $4f$ states. As the transition-metal d band is pushed further below the Fermi level, with increasing band filling, the hybridization strength decreases and leads to a

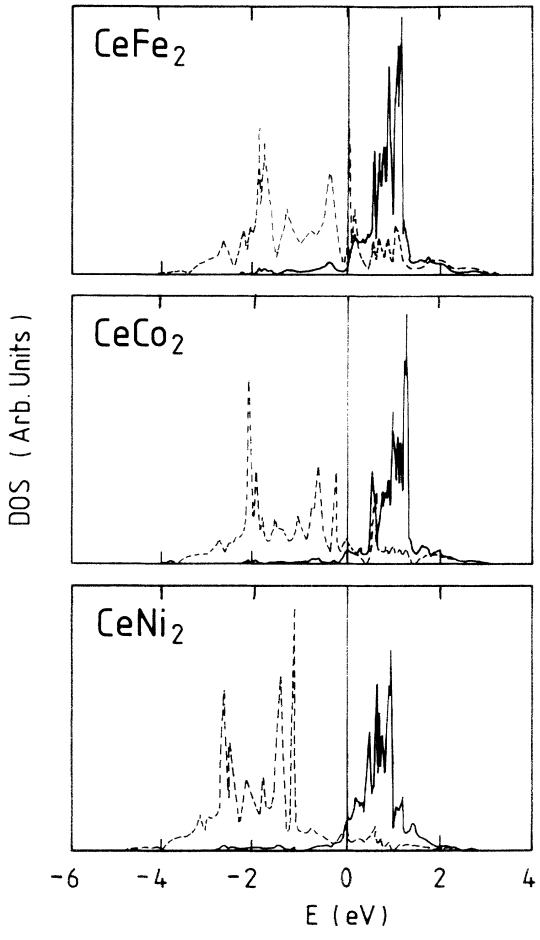

FIG. 1. Calculated one-particle DOS for the Ce $3d$ transition-metal Laves-phase compounds. From top to bottom: $CeFe_2$, $CeCo_2$, and $CeNi_2$. The full line corresponds to the cerium $4f$ states, whereas the dashed line is the ligand d states. The Fermi energy is at zero and is marked by a vertical line. The energy units are in eV while arbitrary units have been used for the DOS.

narrowing also of the cerium $4f$ states. This has drastic consequences, since it is the strength of this hybridization that governs the amount of $4f$ character that is mixed into the major complex of the transition-metal DOS below E_F. The subtle balance between $4f$-$3d$ hybridization and band filling are well accounted for by *ab initio* LDA calculations: Among the cerium compounds, it leads to the magnetism in $CeFe_2$. In a similar way electronic-structure calculations[30,31] for the Laves-phase uranium compounds UFe_2, UCo_2, and UNi_2 show that the decreasing $5f$-$3d$ hybridization, as the $3d$ band gets filled, is responsible for the magnetism in both UFe_2 and UNi_2. In the first of these compounds, UFe_2, the $5f$-$3d$ hybridization is quite strong, and it is the iron states that mainly are responsible for the magnetic instability. With increasing nuclear charge, when proceeding to UCo_2 and UNi_2 the $3d$ band is lowered in energy leading to a decreased hybridization strength and a narrowing of the $5f$ states. In contrast to $CeNi_2$, however, UNi_2 with a filling of 2.7 $5f$ electrons into the $5f$ orbitals is forced to occupy the main peak of the relatively narrow $5f$ states, and this then leads to a high DOS at the Fermi energy, and, therefore, a magnetic instability. So in these compounds, detailed hybridization and band filling effects lead to iron driven $3d$ magnetism in UFe_2, $5f$ driven magnetism in UNi_2, while UCo_2 is nonmagnetic. The same trend of behavior is apparent for $CeFe_2$-$CeNi_2$, where $CeFe_2$ is magnetic due to iron $3d$ states while $CeCo_2$ is not. $CeNi_2$

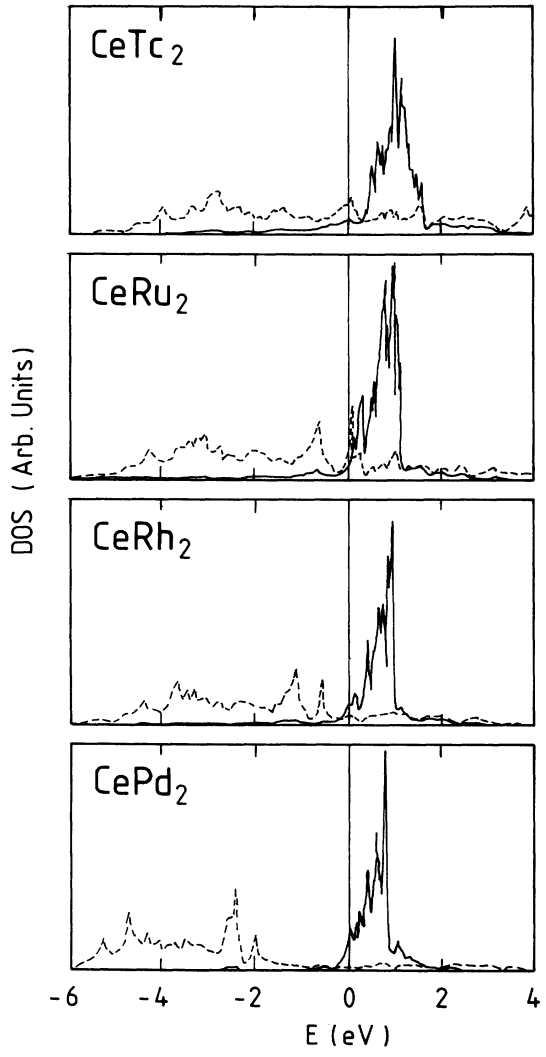

FIG. 2. Calculated one-particle DOS for the Ce $4d$ transition-metal Laves-phase compounds. From top to bottom: $CeTc_2$, $CeRu_2$, $CeRh_2$, and $CePd_2$. The full line corresponds to the cerium $4f$ states, whereas the dashed line is the ligand d states. The Fermi energy is at zero and is marked by a vertical line. The energy units are in eV while arbitrary units have been used for the DOS.

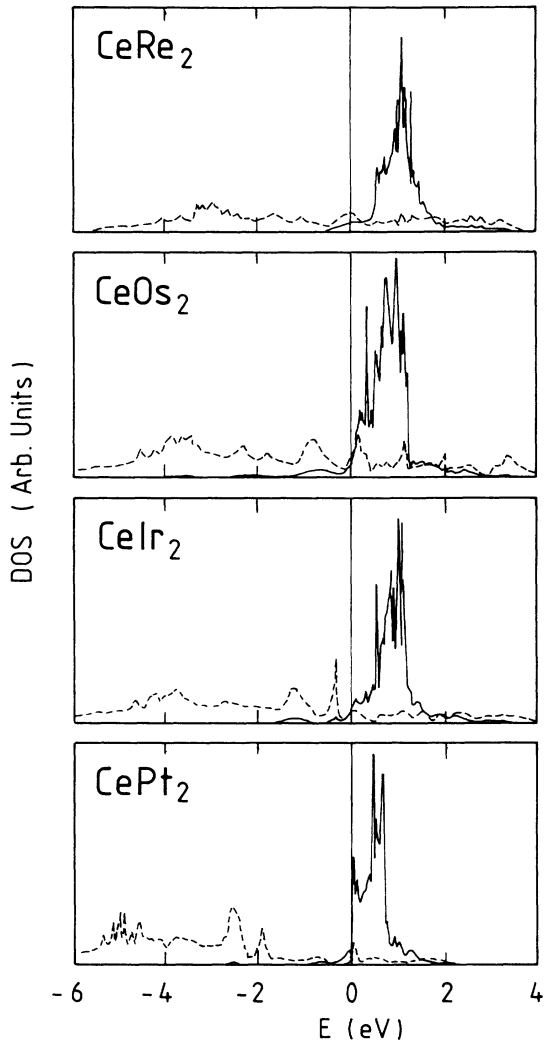

FIG. 3. Calculated one-particle DOS for the Ce $5d$ transition-metal Laves-phase compounds. From top to bottom: $CeRe_2$, $CeOs_2$, $CeIr_2$, and $CePt_2$. The full line corresponds to the cerium $4f$ states, whereas the dashed line is the ligand d states. The Fermi energy is at zero and is marked by a vertical line. The energy units are in eV while arbitrary units have been used for the DOS.

does not fully make it to a magnetic state but shows enhanced paramagnetism due to the $4f$ states. As can be seen from Figs. 2 and 3, the same general trend can also be inferred from the CeA_2 compounds where A denotes a $4f$ or a $5d$ transition-metal atom. For these compounds, however, the $4d$ and $5d$ bands are broader than the $3d$ bands, and thus magnetism is not even expected for the iron group compounds (i.e., $CeRu_2$ and $CeOs_2$).

Concerning the $3d$ compounds $CeFe_2$, $CeCo_2$, and $CeNi_2$ we obtain, in agreement with previous work,[17] the correct lattice constant for all the three elements with an anomalous minimum for $CeCo_2$. This can only be achieved by treating the $4f$ states in the same manner as the other valence states, i.e., as itinerant. If the $4f$ electrons are treated as core states the equilibrium volume becomes too large and the minimum in the lattice constant occurs for $CeNi_2$, as it does for the other rare-earth compounds with a localized $4f$ configuration. Previous[19,20] band theoretical studies on the system $CeNi_x$ ($x=1,2,5$) correctly accounted for the equilibrium volume and the susceptibility enhancement in these compounds. Also for these systems, this could only be obtained by treating the $4f$ electrons on the same footing as the other valence electrons, i.e., allowing them to hybridize in the same manner as the more delocalized states of s, p, and d character. On the other hand, a good description of the specific heat cannot necessarily be inferred since this is not a ground-state property but rather depends on the quasiparticle spectrum of the system and is, therefore, outside the domain of density-functional theory.

Among the Laves-phase compounds, only $CeFe_2$ is ferromagnetic, which is also correctly accounted for by band theory. This can be seen from Fig. 1 where our calculated paramagnetic DOS is quite large at the Fermi level. The Stoner criterion is fulfilled, which implies a ferromagnetic instability. For $CeFe_2$ it is mainly the $3d$ states that are responsible for this large state density, and consequently it is the iron states that drive the magnetic instability and not the $4f$ electrons. As a matter of fact, the magnetic moment of $CeFe_2$ is decreased with approximately one Bohr magneton as compared with the other rare-earth Laves-phase compounds, this being a direct consequence of the contribution of one $4f$ electron to the conduction band with opposite spin direction relative to the spin direction of the $3d$ electrons. Moreover, in $CeFe_2$ the moments on Ce and Fe are antiparallel only as a result of the delocalization of the $4f$ electrons, as the orbital contribution is almost quenched by band formation. In Fig. 4(a) the position of the $3d$ and $4f$ bands are given. Here A, B, and C denotes the top, bottom, and center of the bands, respectively, as defined by the Wigner-Seitz[32] rule. It is clear that with increasing number of $3d$ electrons the center of the $3d$ band is lowered and the corresponding increase of the energy mismatch between the $3d$ and $4f$ levels leads to a narrowing of the $4f$ states. This increased energy separation leads to a hybridization pseudogap (a region with low DOS) between the bonding and antibonding regions of the spectrum. For $CeCo_2$ and $CeNi_2$ the Stoner criterion is not fulfilled, since the Fermi level is situated in the pseudogap region of the DOS (compare Fig. 1), and the simple Stoner picture predicts these compounds to be nonmagnetic in agreement with experiment.

From what has been said it is clear that it is the $4f$-Ad hybridization strength that determines the amount of f character close to the Fermi level. If this hybridization is strong as in $CeFe_2$ (or extremely strong as will be seen in Secs. III and IV to be the case for $CeRh_3$) a hybridization tail of $4f$ character extends several eV below E_F into the bonding part (which is composed of mainly Ad character) of the band structure. Still, even though this tail has an extremely low DOS, one cannot infer that cerium is in a tetravalent state, since this hybridization tail contains a total of more than one $4f$ electron. From our calculations we have found that the total $4f$ charge increases with increasing hybridization strength. This is quite consistent with a band picture of the $4f$ electron, since one could expect the number of $4f$ electrons to differ significantly from one when the hybridization is so strong that the Coulomb repulsion energy is substantially reduced. When this is the case, a description where the bands and the Fermi energy are determined solely by the number of conduction electrons is appropriate. This is the manner in which LDA takes strong correlations into account, since if an orbital is highly localized the total energy will depend more strongly on the occupation of that orbital than if it is weakly correlated. As the hybridization strength decreases the hybridization tail weakens and the $4f$ states become narrower. Since the total $4f$ charge must remain approximately constant due to the large Coulomb energy of the $4f$ orbital (Hubbard U effect) the main peak of the $4f$ DOS is forced to become occupied. This moving of the Fermi level into the main $4f$ peak of the DOS and the suppression of the hybridization tail is seen to occur in the Laves-phase compounds CeA_2. For the compounds where A denotes a $3d$ element this effect is quite noticeable as we proceed from $CeFe_2$ to $CeNi_2$. For the $4f$ or $5d$ elements (Figs. 2 and 3) this effect is even more pronounced.

For the $4d$ and $5d$ compounds the main difference from the $3d$ systems are the broader d bands. According to the Wigner-Seitz rule [see Figs. 4(b) and 4(c)] the $4d$-band width is approximately 11 eV for $CeTc_2$ and drops linearly to 7 eV for $CePd_2$. The corresponding bandwidths for the $5d$ bands are approximately 13 and 8 eV. In $CeFe_2$ the $3d$-band width is 6 eV, and in $CeNi_2$ approximately 4.5 eV [Fig. 4(a)]. In order to investigate the hybridization strength between the $4f$ states of cerium and the d states of the transition metal it is instructive to study Fig. 4. In the beginning of each of the series studied here (the Mn and Fe group compounds), the $4f$ band lies in the region between the center (C parameter) and the top (A parameter) of the transition-metal d band. This leads to a rather strong hybridization between the f and the d states. As we increase the number of d electrons, i.e., proceed to the right in these figures, the center and top of the d bands sink in energy. For the Ni group compounds the d states have dropped so much in energy that the top of the d band just intersects the bottom of the $4f$ band.

This is the reason for the substantial reduction of the hybridization strength and the associated narrowing of the $4f$ band. Comparing $CeNi_2$, $CePd_2$, and $CePt_2$, the top of the d band can be seen to be just below the bottom of the $4f$ band in $CeNi_2$, just above it in $CePd_2$, and close to the top of the $4f$ band in $CePt_2$. This is due to the fact that the d bands get broader with increasing principal quantum number. This then implies that the hybridization strength should be largest in $CePt_2$, since here the $4f$ band is still in between the center and the top of the $5d$ band. However, there is another competing effect. Since the d DOS close to the f DOS is much larger in the $3d$ compounds than in the $4d$ and $5d$ compounds, one could infer that the hybridization strength should be largest for the cerium-$3d$ compounds. These two effects do seem to more or less cancel one another. Actually from the DOS in Figs. 1–3 the hybridization seems to be stronger for the $3d$ compounds in Fig. 1. In the end of the series the main peak of the $4f$ DOS gets occupied for $CePd_2$ and $CePt_2$. When the main peak of a narrow DOS is forced to become occupied, a magnetic instability of the Stoner type is expected. For $4f$ states, however, it is often inferred that this signifies the breakdown of a one-electron picture. For these cases, a significantly more extended investigation, such as a SIC calculation, would be much preferred over the simple Stoner criteria approach used here.

III. THE $AuCu_3$ COMPOUNDS

Among the cerium-transition-metal compounds, only $CeRh_3$, $CePd_3$, and $CePt_3$ form in the relatively simple cubic $AuCu_3$ structure. $CeCo_3$ and $CeNi_3$ form in different and more complicated hexagonal structures. $CeIr_3$ also exists, but forms in the same structure as $CeNi_3$. Among these systems, $CePd_3$ is a mixed-valent system[33] (often characterized by a Kondo temperature close to that of γ-cerium). As was briefly noted in the introduction this latter feature is quite interesting, since the similar compound UPd_3 is a local-moment system. Previous band-structure calculations[34] on the system of uranium compounds UA_3 (A = Tc, Ru, Rh, and Pd) characterized the localization of the $5f$ electrons in UPd_3 as being due to the drastic $5f$-band narrowing that occurs when proceeding from URh_3 to UPd_3. This was shown to be due to the decreased hybridization between the $5f$ and $4d$ bands as the latter becomes filled. Therefore, by comparison, one would expect $CePd_3$ to be a localized $4f$ system. Actually, $CePd_3$ is characterized as a mixed-valent system and, therefore, the energy difference be-

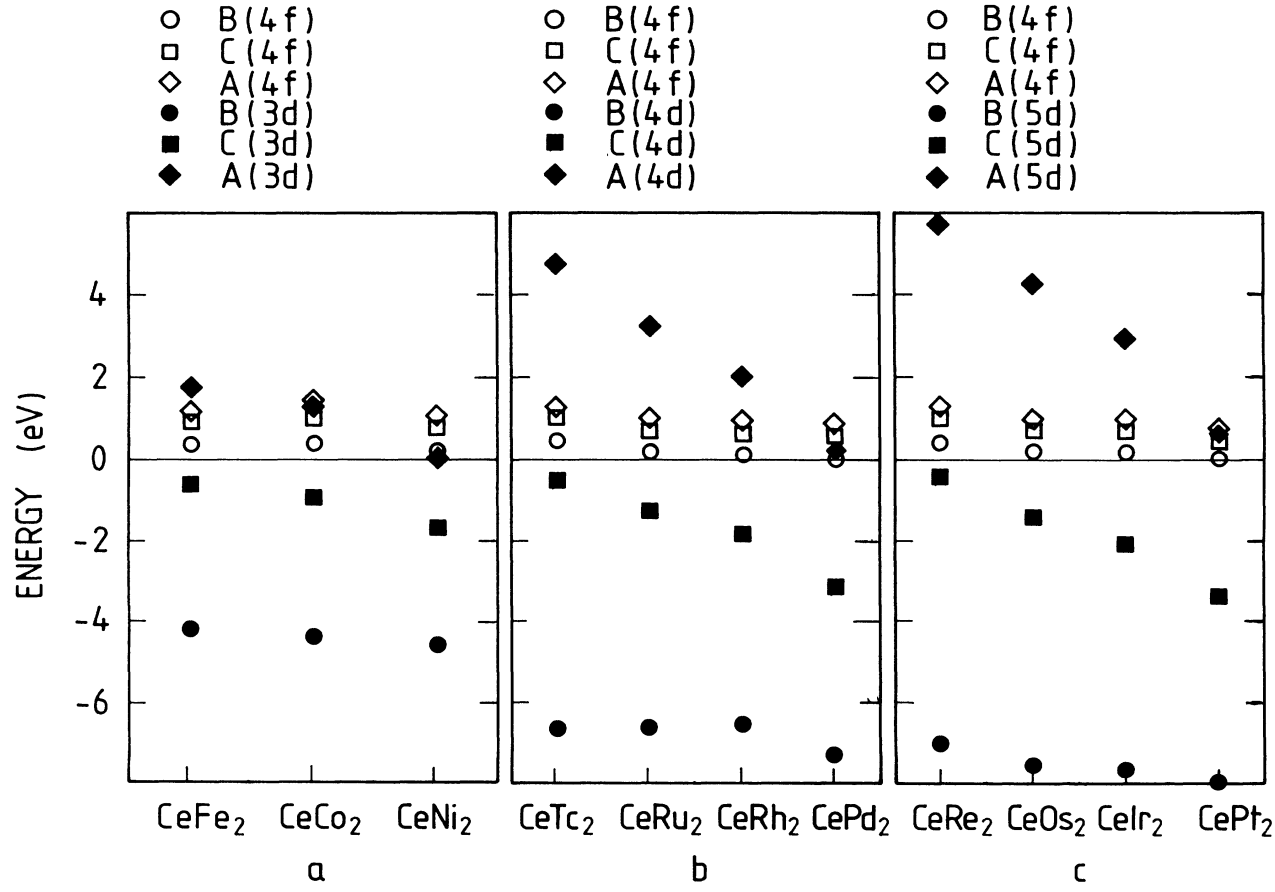

FIG. 4. Bottom (B), center (C), and top (A) of the $3d$ and $4f$ bands in (a) $CeFe_2$, $CeCo_2$, and $CeNi_2$, (b) $CeTc_2$, $CeRu_2$, $CeRh_2$, and $CePd_2$, and (c) $CeRe_2$, $CeOs_2$, $CeIr_2$, and $CePt_2$. The energy units on the vertical axis are eV and the Fermi energy is at zero.

tween the trivalent and tetravalent configurations is much smaller in this compound than in UPd_3. UPd_3 forms in a more complicated hexagonal crystal structure than the other cubic compounds in the series, but this is not believed to be crucial for the localization of the $5f$ electrons in this compound. Further detailed theoretical and experimental studies are needed in order to get a full understanding of these two complicated systems.

$CeRh_3$, on the other hand, differs quite substantially from $CePd_3$. $CeRh_3$ has previously[35] been characterized as being in a tetravalent state, but this is not at all supported, neither by PE spectroscopy experiments[36] nor by our calculations. Indeed, we calculate the number of $4f$ electrons to be approximately 1.6. This is actually larger than in any of the above-mentioned compounds. (In cerium metal our calculations give about 1.1 $4f$ electrons.) These numbers, however, should be used with some caution since they clearly depend on both the division of space into interstitial and muffin-tin regions and on the basis representation used. Experimentally,[37] the susceptibility of this compound is almost temperature independent with an unusually low value. This suggests normal Pauli paramagnetic behavior. It is also interesting to note that $CeRh_3$ has a much smaller lattice constant than $CePd_3$, suggesting this compound to be quite different from $CePd_3$. It is quite likely that $4f$ orbitals are occupied in this compound and this leads to the conclusion that the $4f$ electrons must take an active part in the cohesion. From the DOS seen in Fig. 5, the hybridization tail of $CeRh_3$ is extremely flat around the Fermi energy. This is also true for the corresponding cerium-$5d$ compounds seen in Fig. 6 (except for $CePt_3$). Actually

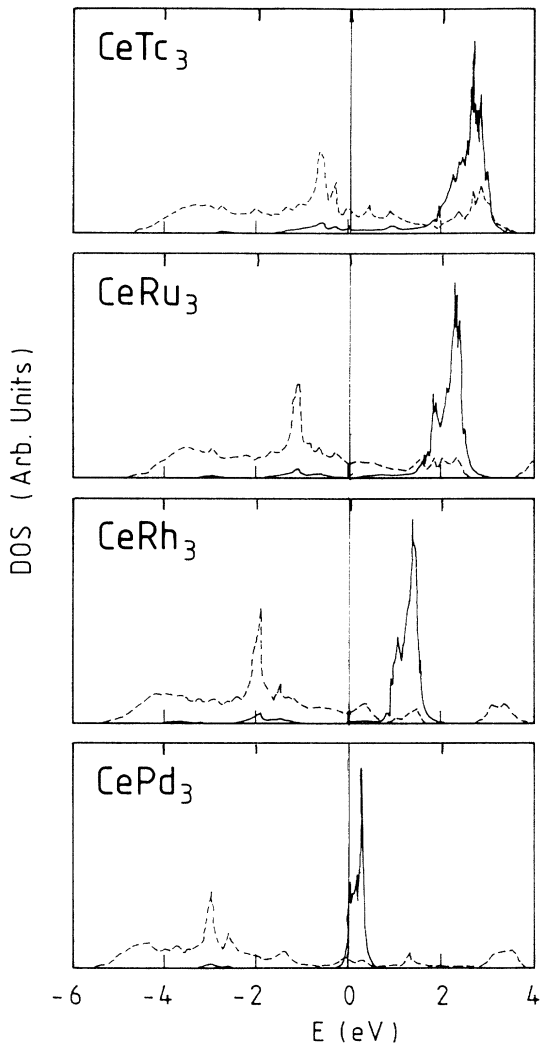

FIG. 5. Calculated one-particle DOS for the Ce $4d$ transition-metal compounds forming in the $AuCu_3$ type structure. From top to bottom: $CeTc_3$, $CeRu_3$, $CeRh_3$, and $CePd_3$. The full line corresponds to the cerium $4f$ states, whereas the dashed line is the ligand d states. The Fermi energy is at zero and is marked by a vertical line. The energy units are in eV while arbitrary units have been used for the DOS.

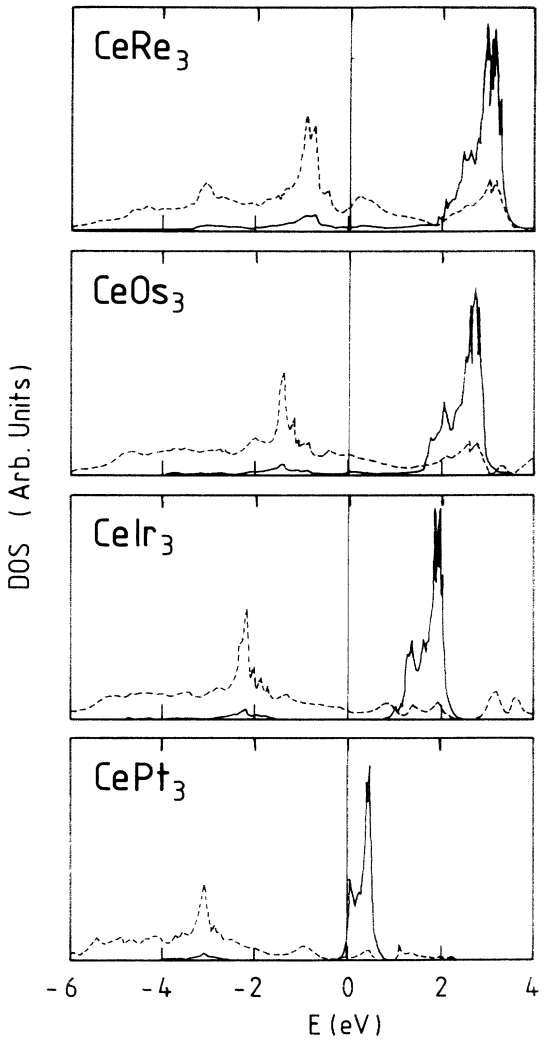

FIG. 6. Calculated one-particle DOS for the Ce $5d$ transition-metal compounds forming in the $AuCu_3$ type structure. From top to bottom: $CeRe_3$, $CeOs_3$, $CeIr_3$, and $CePt_3$. The full line corresponds to the cerium $4f$ states, whereas the dashed line is the ligand d states. The Fermi energy is at zero and is marked by a vertical line. The energy units are in eV while arbitrary units have been used for the DOS.

the electronic structure around E_F is dominated by d bands in these compounds. It is quite clear that it will be extremely difficult to form a local $4f$ moment under such circumstances.[38]

The compounds preceding $CeRh_3$ and $CePt_3$ do not, unfortunately, exist in the cubic $AuCu_3$ crystal structure. $CeIr_3$ does exist, but in the more complicated hexagonal $CeNi_3$ structure. If these compounds had existed in the $AuCu_3$ structure, one would have been able to make a more thorough experimental analysis of the trend towards localization, e.g., using PE and inverse PE spectroscopy. As discussed in the Introduction, the energy position of the $4f^1$ peak in the BIS spectra of $CeRh_3$ is highly anomalous and one would have liked to compare this peak with the corresponding peak in the compounds preceding $CeRh_3$ in the series, if they had existed. Such a comparison would have helped us to gain information, not only about the electronic structure of $CeRh_3$ but also to get some insight into the general behavior of strongly hybridized cerium systems. However, we expect that *ab initio* calculations might give some insight and thus we made calculations for all the hypothetical CeA_3 compounds (A = Tc, Ru, Rh, Pd, Re, Os, Ir, and Pt) in this cubic structure. Our calculated paramagnetic DOS are presented in Figs. 5 and 6. The most obvious thing to note here is the drastic increase of the hybridization strength as compared with the Laves-phase compounds discussed in the previous section. This is mainly caused by the increased coordination number of the cerium atom in this structure as compared to CeA_2 structured compounds discussed in Sec. III. Because of the increased $4f$-ligand d hybridization strength, as compared with the Laves phases, the $4f$-band center moves further away from E_F. The hybridization is stronger in the $5d$ series than in the $4d$ series of compounds, leading to a more pronounced upward shift in the position of the center of the $4f$ band in the former series. Why this is so can be inferred by comparing Figs. 7(a) and 7(b) where the band positions have been plotted similarly to what was done for the Laves phases in the preceding section. The transition-metal $4d$ bandwidth for the $AuCu_3$ compounds can be seen to decrease from 11 eV in $CeTc_3$ to 6 eV in $CePd_3$. For the $5d$ compounds the corresponding numbers are 14 and 8 eV. As was discussed for the Laves-phase compounds, in connection to Fig. 4, the top of the d transition-metal d band cuts the $4f$ band for the $4d$ series, whereas for the $5d$ series the top of the $5d$ band is still above the $4f$ band. Essentially, this is due to the fact that the $5d$ bands are slightly broader than the $4d$ bands. This leads to a stronger hybridization strength for the $5d$ compounds than for the $4d$ compounds. Again, in the end of the series the d band drops in energy quite dramatically, leading to a substantial narrowing of the $4f$ band due to the reduced hybridization strength.

The shift in the $4f$-band center which is clearly recognized is what makes $CeRh_3$ special among those compounds studied experimentally, and, therefore, the next section is devoted to a more detailed investigation of this compound. In Sec. V we will continue discussing the general trend in the $4f$ position suggested by Figs. 5 and 6.

IV. $CeRh_3$: THE MOST HYBRIDIZED CERIUM COMPOUND

For the interpretation of high-energy spectroscopy results, techniques based on the Anderson impurity model

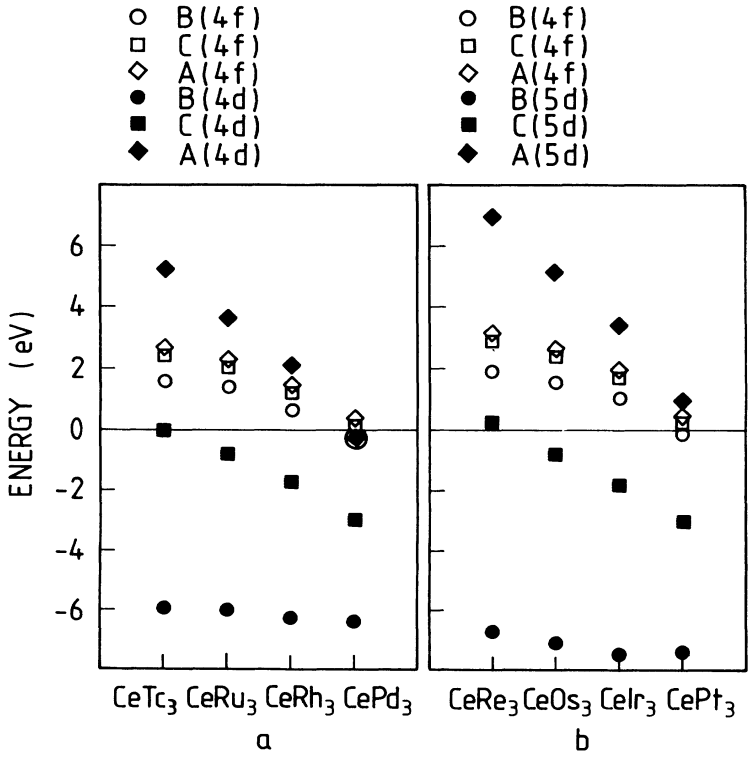

FIG. 7. Bottom (B), center (C), and top (A) of the $4d$ and $4f$ bands in (a) $CeTc_3$, $CeRu_3$, $CeRh_3$, and $CePd_3$ and (b) $CeRe_3$, $CeOs_3$, $CeIr_3$, and $CePt_3$. The energy units on the vertical axis are eV and the Fermi energy is at zero.

have been quite successful. In terms of a few parameters both direct and inverse photoemission spectra for a large class of compounds can be described. However, a recent theoretical prediction[39] that the surface of α-cerium is γ-like, has now been verified experimentally,[40] and since these experimental techniques are surface sensitive a substantial contribution to the PE signal comes from the surface layers. Thus, if the surface has a different electronic structure than the bulk, this difference must be taken into account in order to obtain a correct analysis of the bulk electronic structure. Therefore, a reinterpretation of the PE spectra of cerium compounds becomes necessary. By making use of the energy dependence of the surface sensitivity it has been shown to be possible to separate the bulk and surface signals. This means that bulk cerium is more α-like than previously believed. Whether this should make a band description, which seldom aims to describe photoemission data but rather ground-state properties such as zero-temperature phase diagrams, more appropriate than the impurity model remains to be seen.

$CeRh_3$, the most strongly hybridized cerium system known so far,[41] is naturally a test case for models that attempt to describe the intriguing properties of these compounds. Experimentally,[41] both valence-band photoemission (UPS) and x-ray photoemission (XPS) spectra show features that are difficult to reconcile with a localized description of the $4f$ electron. For example, the strong suppression of the $4f^0$ final-state satellite signal and the absence of the $j=\frac{5}{2}$-$j=\frac{7}{2}$ spin-orbit splitted peaks close to the Fermi energy in the UPS spectra signifies the strength of the $4f$ hybridization in this compound. Inverse photoemission (BIS) shows similar evidence of extremely strong $4f$ hybridization: The $4f^1$ peak is pushed further above E_F than in any other known cerium compound. Moreover, the strength of the $4f^2$ satellite signal is extremely suppressed, actually weaker than a peak of Ce $5d$ character 3–4 eV above E_F.[42] In Fig. 8 we have inserted our calculated state density (with appropriate lifetime and resolution broadening) together with the observed BIS spectra (Ref. 41), and it is seen that our calculated band center for the $4f$ states and its shape agrees remarkably well with the experimentally obtained BIS peak. Also, the calculated Ce $5d$ state density agrees well with the experimental data. In order to fit the BIS spectra with parameters from the SI model comparable magnitudes of the hybridization ($\Delta=1.9$ eV) and correlation ($U=3.2$ eV) parameters has to be used (Ref. 41).

One could then ask to what extent a band picture provides an accurate description. In order for such a picture not be unrealistic, the $4f$ wave function must have a substantial weight at the sphere boundary. In Fig. 9 we thus present the self-consistently calculated $4f$ wave function at three different energies. The curve with the most weight at the sphere boundary (the thickest curve) corresponds to an energy equal to the center of the occupied part of the $4f$ hybridization tail. The curve in the middle is the wave function at the Fermi energy, and the thin line corresponds to the center of the total $4f$ band. The latter wave function is well localized, and corresponds to an atomiclike cerium $4f$ wave function. This orbital is, however, not occupied since its energy is above E_F. The Fermi energy $4f$ wave function has much more weight at

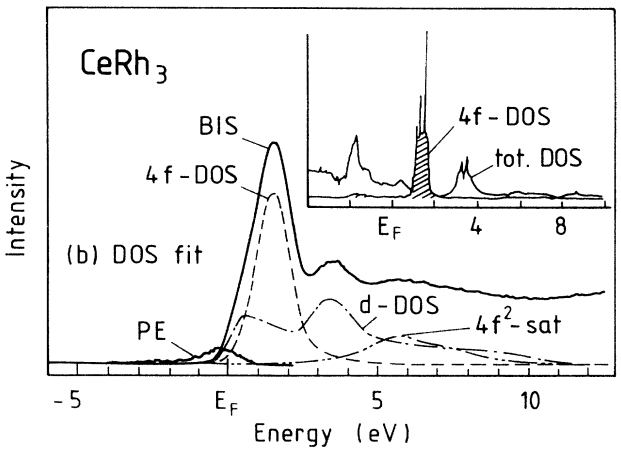

FIG. 8. Inverse photoemission on $CeRh_3$ (from Ref. 41). The major feature at 1.4 eV is the $4f^1$ peak. The peak at ≈ 4 eV has d character. Note the strongly suppressed $4f^2$ final state at ≈ 5–6 eV. We have inserted our calculated $4f$ and Ce $5d$ state densities with appropriate lifetime broadening as well. At the top right-hand corner the self-consistently calculated total DOS is presented (with no broadening). The Fermi energy (E_F) is inserted and the energy units are given in eV. All intensities are in arbitrary units.

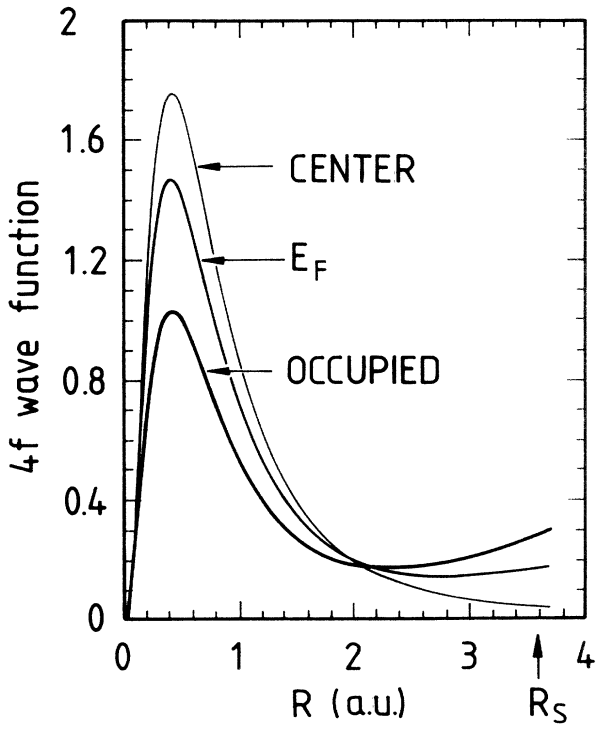

FIG. 9. Calculated cerium $4f$ wave function for $CeRh_3$. The three different curves correspond to different energies. With increasing weight at the Wigner-Seitz radii ($=R_S$) they correspond to the center of the total $4f$ band, the Fermi energy, and the center of the occupied part of the $4f$ band, respectively.

the Wigner-Seitz sphere, and for the "average" occupied wave function (the thickest curve) a substantial overlap with neighboring atoms is found (the Wigner-Seitz radius used is indicated by an arrow in Fig. 9). It is not difficult to imagine this wave function to be part of a bonding band complex. Quite an interesting fact is displayed by Fig. 9. With increasing band energy, the $4f$ wave function contracts substantially. This leads to a smaller weight at the sphere boundary, and a much more pronounced peak closer to the nuclei. Therefore, the corresponding Coulomb repulsion among the $4f$ electrons is expected to increase with increasing band energy. This means that for $CeRh_3$ we have a strongly energy-dependent Hubbard repulsion, being much smaller in the occupied part of the $4f$ band, than above E_F. This fits quite neatly into the arguments of the preceding section on how LDA by self-consistently handles strongly correlated cerium orbitals. If by hybridization effects, as for $CeRh_3$, the $4f$ wave function looks similar to the thickest plotted curve in Fig. 9, then the Hubbard repulsion is substantially reduced and the Hartree term of the total LDA energy functional will not be crucially dependent on the $4f$ occupation. Thus such a system is similar to the ordinary transition metals, where the Fermi level is simply given by the number of total conduction electrons, and, therefore, the $4f$ occupation may differ significantly from a localized integer value (in this case one). On the other hand, if the $4f$ orbital looks like the localized center of band wave function in Fig. 9, the Hartree energy will be much larger. Then the total $4f$ occupation is limited within a narrow range, and consequently the $4f$ peak is constrained to be very close to the Fermi energy. Under such circumstances the validity of a one-electron picture is more questionable. For a given compound, the case is settled by self-consistency.

V. A BAND PICTURE FOR THE $4f^1$ POSITION IN CERIUM BIS SPECTRA

In LDA calculations the occupation numbers of the various orbitals in an intermetallic compound are not substantially changed from the values they have in the pure metallic state. For example, the number of iron $3d$ electrons turns out to be roughly 6.6 irrespective of its metallic surrounding. Again, as previously stressed, such numbers are clearly representation dependent, but nevertheless serve as a rough guide. The physical mechanism that gives rise to this behavior is the relatively large Coulomb repulsion of the narrow atomiclike states, which efficiently constrains the occupation numbers of the various orbitals within a limited range. Thus this mechanism is particularly effective for d and f states. Then, in intermetallic compounds the *hybridized* bonding band must have a mixture of different characters in order to keep this charge conservation.

The LMTO Hamiltonian may be cast into the form[43,44]

$$H_{tlm,t'l'm'}=C_{tl}\delta_{tt'}\delta_{ll'}\delta_{mm'}+\Delta_{tl}^{1/2}S_{tlm,t'l'm'}\Delta_{t'l'}^{1/2} ,$$

where the transfer integrals $\Delta^{1/2}S\Delta^{1/2}$ are similar to the Slater and Koster[45] linear combination of atomic orbitals two center integrals (t,l,m label the atom type and angular momentum state) and C is the band center potential parameter. In the case of weak hybridization the number of states of $T=(tlm)$ character that are hybridized into what was, before hybridization, of pure T' character is proportional to $\Delta_T\Delta_{T'}/(C_T-C_{T'})^2$. In terms of this picture we may understand how the center of the $4f$ band is pushed further above the Fermi level, with increasing hybridization, in order to keep the total $4f$ charge roughly constant.

In Secs. II and III we presented figures of the positions of the bands (given by the value of the logarithmic derivative of the corresponding wave function at the sphere boundary) and DOS for the compounds considered. Here we wish to study the general trend of the position of the $4f$ band among those compounds. First, we recognize this position to be essentially equal to the energy of the band center potential parameter (C) in Figs. 4 and 7. That this is so can be seen by comparison with the corresponding plots of the DOS (Figs. 1–3 and 5–6). However, in a BIS experiment the $4f^1$ peak is given with respect to the Fermi energy, and thus the position of this peak depends on band filling. For this purpose it is better to plot the calculated $4f$ band center as the zero of the energy scale, and then plot the position of the center of the transition-metal d band and E_F with respect to this zero. For the Laves-phase compounds this is done in Fig. 10 (for the cerium $3d$, $4d$, and $5d$ compounds, respectively). For the $AuCu_3$ compounds the corresponding plots are given in Fig. 11. From these figures we can directly read off the position of the $4f^1$ peak, as the distance from E_F (denoted by a black dot) to the horizontal line that marks the zero of energy (the $4f$ band center). For the Laves-phase compounds we conclude that this distance varies between 0.3 and approximately 1.0 eV. For the Mn group elements $CeTc_2$ and $CeRe_2$ the Fermi level has to be close to the transition-metal d-band center, since here the transition-metal d occupation is approximately five. For the $AuCu_3$ structured compounds (denoted here by CeA_3), on the other hand, the hybridization is much larger since the cerium coordination number is larger. In a simple hybridization model the unhybridized bands mix and push apart as a consequence of the mixing, in the notation given above, first-order perturbation theory suggests this splitting between the bands to be proportional to $\Delta_T\Delta_T/(C_T-C_{T'})$. Now, in the calculational loop, these mixings and shifts of bands are determined self-consistently. Nevertheless, we may understand why the center of the transition-metal d band is so much further below the $4f$ band in the CeA_3 compounds than in the corresponding Laves-phase compounds from this expression. For the late elements $CePd_3$ and $CePt_3$ the d-band filling is almost complete and thus the Fermi level is close to the $4f$-band center. For the Mn group compounds $CeTc_3$ and $CeRe_3$, as for the corresponding Laves-phase compounds, E_F is close to the center of the transition-metal band. But since the hybridization induced splitting of the Ad and Ce $4f$ levels is much larger for this structure than for the Laves phase, the energy distance to the center of the $4f$ band, from the center of the Ad band is much larger as well. This explains the drastic increase in the calculated energy distance between the $4f$ and ligand

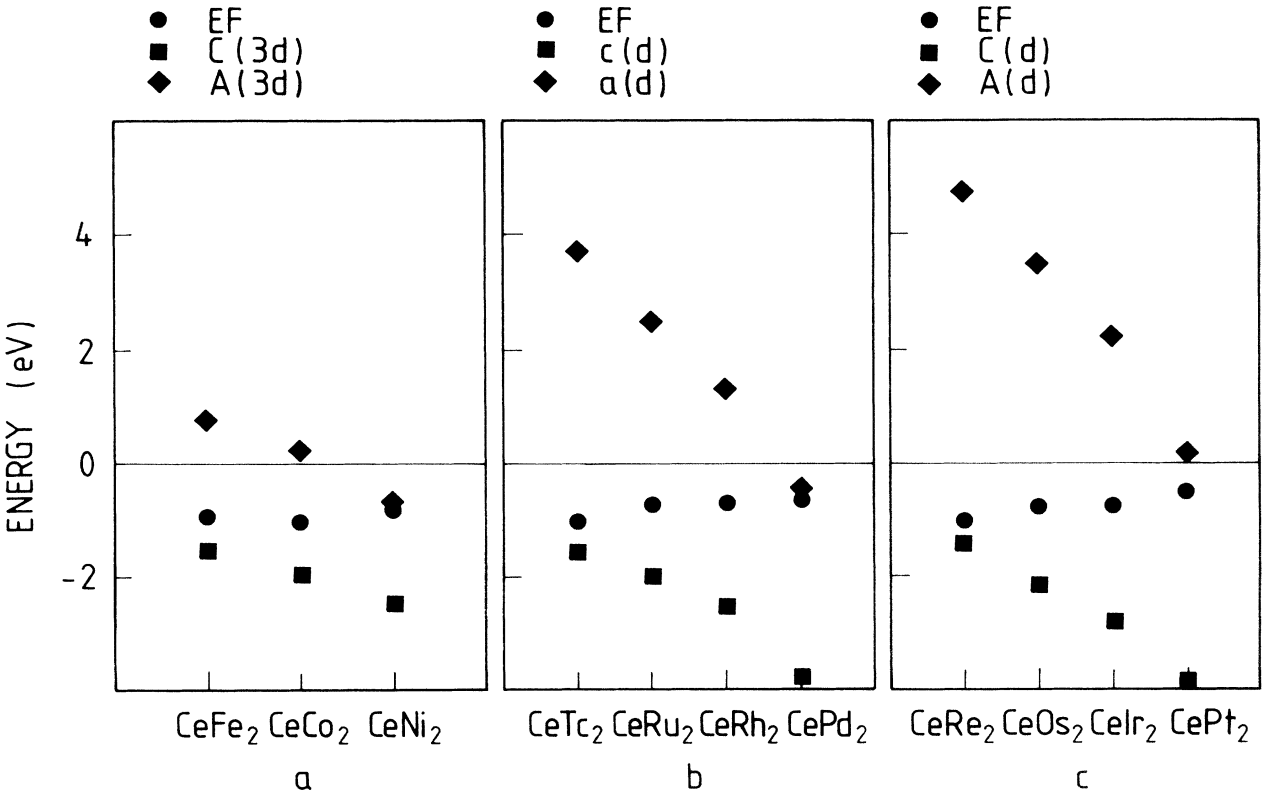

FIG. 10. Changes in position of bands (the energy of the $4f$ level is equal to zero) for the Laves-phase compounds. The energy scale is in eV: (a) $CeFe_2$, $CeCo_2$, and $CeNi_2$, (b) $CeTc_2$, $CeRu_2$, $CeRh_2$, and $CePd_2$, and (c) $CeRe_2$, $CeOs_2$, $CeIr_2$, and $CePt_2$.

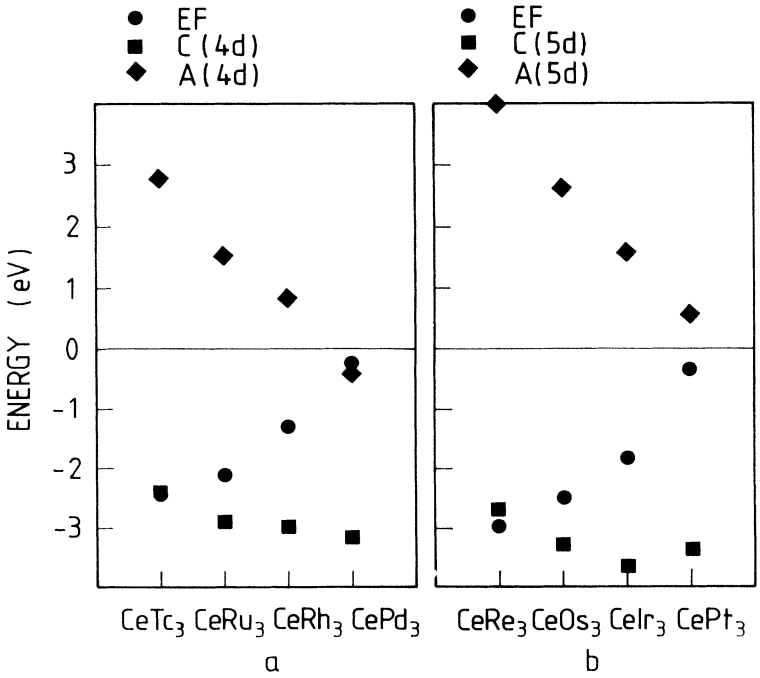

FIG. 11. Changes in position of bands (the energy the $4f$ level is equal to zero) for the $AuCu_3$ phase compounds. The energy scale is in eV: (a) $CeTc_3$, $CeRu_3$, $CeRh_3$, and $CePd_3$, and (b) $CeRe_3$, $CeOs_3$, $CeIr_3$, and $CePt_3$.

d band in these compounds, as well as the corresponding increase in the $4f^1$ peak position as one proceeds from $CePd_3$ to $CeRh_3$.

From the discussions in Secs. II and III it is clear that the hybridization strength between the $4f$ states and the d states of the ligand increases with the number of nearest-neighbor atoms that cerium has. Moreover, the compounds in the $5d$ series often hybridize more strongly with the $4f$ states than the corresponding $4d$ compounds do. With this in mind, compounds formed by Ce and atoms to the left of Pt in the Periodic Table would be ideally suited for the investigation of $4f$ delocalization. Of the possible compounds, only $CeIr_3$ and $CeIr_5$ exists to our knowledge. The latter compound forms in the cubic $AuBe_5$ structure, whereas the former forms in a more complicated hexagonal structure. We, therefore, performed self-consistent calculations for $CeIr_5$ in the $AuBe_5$ phase and our paramagnetic DOS are presented in the middle panel of Fig. 12. (The DOS of $CeIr_3$ has been inserted in the upper panel of Fig. 12 for comparison.) The $4f$-$5d$ hybridization does not seem to be larger in this compound than in $CeIr_3$ discussed in Sec. III. This is due to the fact that the $AuBe_5$ structure has two different Be sites. The Be(I) site is closest to the cerium atom, but there is only one atom of this type in the unit cell. There are four atoms of type Be(II), but they are further away from the cerium atom than the Be(I) site is, and this explains why the hybridization strength is not as strong in this compound as one might have expected from the outset. In this respect, the hexagonal $CaCu_5$ structure is a more suitable structure for the purpose of finding a compound with an unusually large $4f$-ligand d hybridization strength, since there is only one type of Cu site in the unit cell. Even though $CeIr_5$ is not thermodynamically stable in this structure, we have performed calculations for this hypothetical compound and the DOS is presented in the bottom of Fig. 12. It is clear that the hybridization strength is much larger here than for $CeIr_5$ in the $AuBe_5$ structure. Compared with the $AuCu_3$ structure (top in Fig. 12), the hybridization strength is of comparable magnitude.

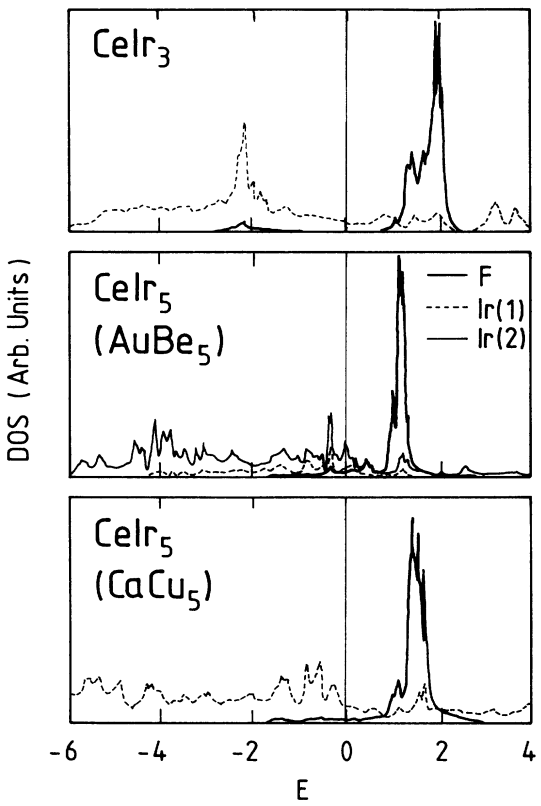

FIG. 12. Calculated one-particle DOS for $CeIr_3$ in the $AuCu_3$ structure (top), $CeIr_5$ in the $AuBe_5$ (middle), and the $CaCu_5$ structure (bottom). The full line is the $4f$ state DOS, whereas the dashed line corresponds to the Ir $5d$ states. All energy units are in eV and the Fermi energy is marked with a vertical line at $E=0$.

VI. CONCLUSIONS

In this paper, we have discussed the potential of using *ab initio* LDA calculations in order to describe the electronic structure of a number of cerium intermetallic compounds. There is no doubt that crystallographic phase diagrams can be described with a very high degree of accuracy and also ground-state magnetic properties can be accounted for. As an example of this, we mention that band theory gives the correct lattice constants for $CeFe_2$, $CeCo_2$, and $CeNi_2$,[17] especially accounting for the anomalous minimum for $CeCo_2$. This is only achieved by including the $4f$ electrons in the band structure. For $CeRh_3$ the correct lattice constant is obtained when the cerium $4f$ electrons are included in the band structure. For the magnetic properties, the ferromagnetism in $CeFe_2$ is well accounted for,[17] and its magnetic moment compares favorably with experiment. The magnetic properties of the hexagonal ferromagnet $CeCo_5$ are also well described by band theory.[19,46] Such results give substantial support for the correctness of $4f$ delocalization in these compounds.

For the Pd and Pt compounds the situation is more complex. For example, $CePd_3$ is often considered as a mixed-valence system. Our paramagnetic calculation gives an equilibrium lattice constant that is far too small. Since the equilibrium volume of the preceding compound $CeRh_3$ is well accounted for, it is concluded that LDA fails for $CePd_3$. Actually, this compound is likely to be a true mixed-valent system. We have discussed the similarities and differences between $CePd_3$ and UPd_3. The latter compound has a localized ($5f^2$) configuration. Previous calculations[34] accounted for this localization of uranium $5f$ electrons as being due to a drastic decrease of the $5f$-$4d$ hybridization when the bonding (mostly $4d$) band gets filled. This leads to a significant narrowing of the calculated f-band width, and the fulfillment of a Stoner criterion. In this respect our calculations for the Ce-Pd and Ce-Pt systems are similar to the calculations for UPd_3.

From the $4f$-band point of view, $CeRh_3$ is well behaved. It is also widely recognized as the most strongly hybridized cerium system. This is apparent for example when probing with core-level spectroscopy (XPS) and

valence-band photoemission. These experimental techniques emphasize the localized character to a larger extent than the band character, since the $4f$ final state of the PE process shows a more pronounced localized character than the initial state does. In $CeRh_3$, however, the valence-band 2-eV satellite is almost completely suppressed, and the spectrum close to the Fermi level is almost flat. In nickel metal, even though PE spectroscopy reveals a 6-eV valence-band satellite, there is no doubt that the appropriate starting point is a band description of the d electrons. It is commonly believed that such effects can then be accounted for by adding local corrections to the band Hamiltonian.[47] The BIS spectrum of $CeRh_3$ is most interesting with a $4f^1$ final state peak as high as 1.4 eV above E_F. Such a high value for the position of the $4f^1$ peak is not possible to reconcile within a Kondo picture. There is some ambiguity concerning the accuracy of the experimental data, a value of 1.0 eV has been quoted (see Ref. 27) but also this value is very large. The $4f^2$ final state is observed to be strongly suppressed and other details in the spectra can be explained as being due to transitions into more delocalized d states.[40] As shown in Ref. 41 the BIS spectra for $CeRh_3$ clearly marks the limits of the applicability of the SI model. For example the hybridization (Δ) and correlation (U) parameters used to describe the spectra differ significantly from other cerium compounds, and they are not consistent with those to be derived from the XPS data on $CeRh_3$. Since U and Δ are almost equal, a band description could be more favorable than one based on an impurity model.

In Fig. 13 we have plotted the position of the $4f$ band as obtained from both BIS spectra (the y axis) and our calculations (the x axis). The $x=y$ line would thus correspond to perfect agreement between a one-electron picture and experiment. As can be seen, the values for the Laves phases are scattered around the $x=y$ line. Best agreement between one-electron theory and BIS data are actually found for $CeRh_3$, and this is not surprising considering this compound to be the far most delocalized $4f$ system studied experimentally. The experimental values are unfortunately subject to rather large error bars. This is particularly true for $CeRu_2$ where also a value of approximately 0.4 eV can be inferred (Ref. 26). Better resolution is needed here to clarify the situation.

The $4f^1$ peak seen in BIS spectra has been shown to be part of a trend. By performing calculations for a set of hypothetical as well as existing cerium compounds forming in the $AuCu_3$ structure this $4f^1$ position may be seen to be a natural consequence of the changing strength of the $4f$-$4d$ (or $4f$-$5d$) hybridization, as the series is traversed. Quite interesting is that the same effect occurs also if one keeps the same constituent atoms in the compound, but changes their ratio with respect to the cerium content. In Ref. 20, e.g., DOS for $CeNi_x$ ($x=1,3,5$) are plotted which clearly show the $4f$ position moving further above E_F as the nickel content is increased. From these plots this position may be inferred to be 0.5, 0.8, and 1.0 eV for CeNi, $CeNi_2$, and $CeNi_5$, respectively. In Sec. IV we clearly recognized that this peak position was shifted upwards as we went from cerium-$4d$ to cerium-$5d$ compounds. It seems to us that compounds of the type CeA_5 (A is a $4d$ or $5d$ element without a full d band) forming in the $CaCu_5$ structure would be particularly useful to study experimentally by means of inverse photoemission. It would quite likely be an even more delocalized $4f$ system than $CeRh_3$, and as such would be extremely interesting to investigate experimentally to further explore the possibility of $4f$ itinerancy. From the theoretical side, SIC calculations on these more complicated systems (compared to Ce metal) would be desirable. Even though some of the compounds studied in this paper, in particular $CeRh_3$, presumably are more delocalized than α-cerium, the result of explicit SIC calculations would be useful for comparison.

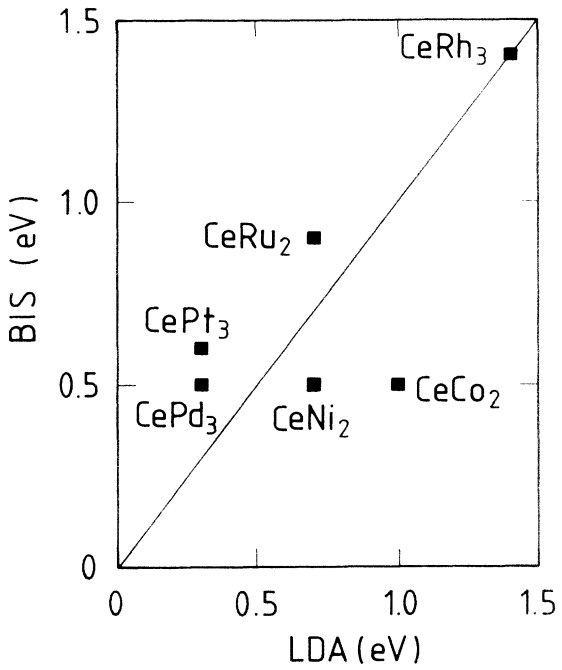

FIG. 13. Plot of the position of the $4f^1$ peak in a diagram with the LDA calculated band center on the x axis, and the position of the $4f^1$ final state as obtained in BIS spectra on the y axis.

ACKNOWLEDGMENTS

Lukas Severin and Börje Johansson are grateful to the Swedish Natural Science Research Council for financial support. Fruitful discussions with Olle Eriksson are acknowledged.

*Present address: Institut für Festkörperphysik, Hochschulstraße 6/8, Technische Hochschule, D-64289 Darmstadt, Fed. Rep. of Germany.

[1]D. C. Koskenmaki and K. A. Gschneidner Jr., in *Handbook of the Physics and Chemistry of Rare Earths*, edited by K. A. Gschneider Jr. and L. Eyring (North-Holland, Amsterdam, 1979), Vol. 1, p. 337.

[2]B. I. Min, H. F. J. Hansen, T. Oguchi, and A. J. Freeman,

Phys. Rev. B **34**, 369 (1986); D. Glötzel, J. Phys. F **8**, L163 (1978); A. Yanese, *ibid.* **16**, 1501 (1986); O. Eriksson, M. S. S. Brooks, and B. Johansson, Phys. Rev. B **41**, 7311 (1990); W. E. Picket, A. J. Freeman, and D. D. Koelling, *ibid.* **23**, 1266 (1981).

[3]B. Johansson, Philos. Mag. **30**, 469 (1974).

[4]J. W. Allen and R. M. Martin, Phys. Rev. Lett. **49**, 1106 (1982); M. Lavagna, C. Lacroix, and M. Cyrot, Phys. Lett. **90A**, 210 (1982).

[5]O. Gunnarsson and K. Schönhammer, Phys. Rev. B **28**, 4315 (1983); J. W. Allen, S. J. Oh, O. Gunnarsson, K. Schönhammer, M. B. Maple, M. S. Torikachvili, and I. Lindau, Adv. Phys. **35**, 275 (1986); J. C. Fuggle, F. U. Hillebrecht, Z. Zolnierek, R. Lässer, C. Freiburg, O. Gunnarsson, and K. Schönhammer, Phys. Rev. B **27**, 7330 (1983).

[6]F. Patthey, J.-M. Imer, W.-D. Schneider, H. Beck, Y. Baer, and B. Delley, Phys. Rev. B **42**, 8864 (1990).

[7]J. R. Schrieffer and P. A. Wolff, Phys. Rev. **149**, 491 (1966).

[8]A. K. McMahan, J. Less-Common Met. **149**, 1 (1989).

[9]H. L. Skriver, Phys. Rev. B **31**, 1909 (1985).

[10]O. Eriksson, J. M. Wills, and A. M. Boring, Phys. Rev. B **46**, 12 981 (1992); J. M. Wills, O. Eriksson, and A. M. Boring, Phys. Rev. Lett. **67**, 2215 (1991).

[11]J. Wittig, Phys. Rev. Lett. **21**, 1250 (1968); F. H. Elliner and W. H. Zachariasen, *ibid.* **32**, 773 (1974); W. H. Zachariasen and F. H. Ellinger, Acta Crystallogr. Sec. A **33**, 155 (1977).

[12]Z. Szotek, W. M. Temmerman, and H. Winter, Phys. Rev. Lett. **72**, 1244 (1994); A. Svane, *ibid.* **72**, 1248 (1994), and references therein.

[13]Y. Baer, in *Handbook on the Physics and Chemistry of the Actinides,* edited by A. J. Freeman and G. H. Lander (North-Holland, Amsterdam, 1984), Vol. 1, p. 271.

[14]See e.g., J. Lawrence and Y.-Y. Chen, in *Theoretical and Experimental Aspects of Valence Fluctuations and Heavy Fermions,* edited by L. C. Gupta and S. K. Malik (Plenum, New York, 1987), p. 169.

[15]M. Norman and D. D. Koelling, in *Handbook of the Physics and Chemistry of the Rare Earths,* edited by K. A. Gschneider Jr. and S. Hüfner (North-Holland, Amsterdam, 1993), Vol. 17, p. 1.

[16]R. C. Albers, A. M. Boring, and N. E. Christensen, Phys. Rev. B **33**, 8116 (1986); R. C. Albers, *ibid.* **32**, 7646 (1985); C. S. Wang, M. R. Norman, R. C. Albers, A. M. Boring, W. E. Picket, H. Krakauer and N. E. Christensen, *ibid.* **35**, 7260 (1987); M. R. Norman, R. C. Alberg, A. M. Boring, and N. E. Christensen, Solid State Commun. **68**, 245 (1988).

[17]O. Eriksson, L. Nordström, M. S. S. Brooks, and B. Johansson, Phys. Rev. Lett. **24**, 2523 (1988).

[18]L. Severin, M. S. S. Brooks, and B. Johansson (unpublished); L. Severin, M. S. S. Brooks, and B. Johansson, Phys. Rev. Lett. **71**, 3214 (1993).

[19]L. Nordström, O. Eriksson, M. S. S. Brooks, and B. Johansson, Phys. Rev. B **41**, 9111 (1990).

[20]L. Nordström, M. S. S. Brooks, and B. Johansson, Phys. Rev. B **46**, 3458 (1992).

[21]L. Nordström, Ph.D. thesis, Uppsala University, 1991.

[22]Especially for strongly correlated f systems, LDA fails badly for calculations of the specific heat, even though ground-state properties such as crystal structure and magnetic moments are remarkably well predicted. For these systems the charge excitations, as revealed, e.g., in PE spectroscopy experiments, are separated from the spin excitations. For low-temperature properties the latter is completely dominant and is responsible for the enhancement of the specific heat. Herein lies the failure of LDA, since it is not capable of this separation of the excitation spectra. For a good discussion, see e.g., P. Fulde, *Electron Correlations in Molecules and Solids,* Springer Series Solid-State Sciences Vol. 100 (Springer, Berlin, 1991).

[23]Y. Baer and W. D. Schneider, in *Handbook of the Physics and Chemistry of Rare Earths,* edited by K. A. Gschneider Jr., L. Eyring, and S. Hüfner (North-Holland, Amsterdam, 1987), Vol. 10, p. 1.

[24]M. R. Norman, D. D. Koelling, A. J. Freeman, H. J. F. Hansen, B. I. Min, T. Oguchi, and L. Ye, Phys. Rev. Lett. **53**, 1673 (1984); A. J. Freeman, R. I. Min, and M. R. Norman, in *Handbook of the Physics and Chemistry of Rare Earths* (Ref. 23), Vol. 10, p. 165.

[25]C. Laubschat, E. Wescke, C. Holtz, M. Domke, O. Streibel, and G. Kaindl, Phys. Rev. Lett. **69**, 1792 (1992).

[26]F. U. Hillebrecht, C. Fuggle, G. A. Zawatzky, M. Campagna, O. Gunnarsson, and K. Schönhammer, Phys. Rev. B **30**, 1777 (1984); F. U. Hillebrecht and M. Campagna, in *Handbook of the Physics and Chemistry of Rare Earths* (Ref. 23), Vol. 10, p. 425.

[27]In a private communication, Y. Baer provided a value of 1.0 eV for $CeRh_3$. Although this is lower than the data from Ref. 41, it is still anomalously high compared with the data for the other cerium compounds. See also discussion in D. Malterre, M. Grioni, Y. Baer, L. Braicovich, L. Duò, P. Vavassori, and G. L. Olcese, Phys. Rev. Lett. **73**, 2005 (1994); E. Weschke, C. Laubschat, A. Höhn, M. Domke, G. Kaindl, L. Severin, and B. Johansson, *ibid.* **73**, 2006 (1994).

[28]O. K. Andersen, Phys. Rev. B **12**, 3060 (1975).

[29]U. von Barth and L. Hedin, J. Phys. C **5**, 1629 (1972).

[30]L. Severin, L. Nordström, M. S. S. Brooks, and B. Johansson, Phys. Rev. B **44**, 9392 (1991).

[31]O. Eriksson, B. Johansson, H. L. Skriver, and M. S. S. Brooks, Physica B **144**, 32 (1986); M. S. S. Brooks, O. Eriksson, and B. Johansson, Phys. Scr. **35**, 52 (1987).

[32]According to this rule of thumb the bottom (B) and top (A) of a band of l character is given by the condition that the logarithmic derivative D_l of the corresponding wave function equals $D_l=0$ and $D_l=-\infty$, respectively, at the sphere boundary. These conditions correspond to the bonding and antibonding solutions of the hydrogen molecule. The center of the band is, according to the same rule, defined by $D_l=-l-1$. This logarithmic derivative is appropriate for a resonance scattering state.

[33]D. Malterre, M. Grioni, P. Weibel, B. Dardel, and Y. Baer, Phys. Rev. Lett. **68**, 2656 (1992), and references therein.

[34]O. Eriksson, B. Johansson, M. S. S. Brooks, and H. L. Skriver, Phys. Rev. B **38**, 12 858 (1988); **40**, 9508 (1989).

[35]G. L. Olcese, J. Phys. (Paris) Colloq. **40**, C5-334 (1979); J. G. Sereni, G. L. Olcese, and C. Rizzuto, *ibid.* **40**, C5-337 (1979).

[36]C. Laubschat, W. Grentz, and G. Kaindl, Phys. Rev. B **36**, 8233 (1987).

[37]J. P. Kappler, P. Lehmann, G. Schmerber, G. Nieva, and J. G. Sereni, J. Phys. (Paris) Colloq. **49**, C8-721 (1988).

[38]L. Severin, Phys. Rev. B **46**, 7905 (1992).

[39]O. Eriksson, R. C. Albers, A. M. Boring, G. W. Fernando, I. G. Hao, and B. R. Cooper, Phys. Rev. B **43**, 3137 (1991).

[40]E. Wescke, C. Laubschat, C. T. Simmons, M. Domke, O. Streibel, and G. Kaindl, Phys. Rev. B **44**, 8304 (1991).

[41]E. Wescke, C. Laubschat, R. Ecker, A. Höhr, M. Domke, G. Kaindl, L. Severin, and B. Johansson, Phys. Rev. Lett. **69**, 1792 (1992).

[42]See also, F. U. Hillebrecht, J. C. Fuggle, G. A. Sawatzky, and R. Zeller, Phys. Rev. Lett. **51**, 1187 (1983).

[43]O. K. Andersen, W. Klose, and H. Nohl, Phys. Rev. B **17**, 1209 (1978).

[44]M. S. S. Brooks, O. Eriksson, and B. Johansson, J. Phys. Condens. Matter **1**, 5681 (1989).

[45]J. C. Slater and G. F. Koster, Phys. Rev. **94**, 1498 (1954).

[46]Review articles on the calculated magnetic properties and electronic structure of rare-earth and actinide compounds may be found in, e.g., B. Johansson, O. Eriksson, L. Nordström, L. Severin, and M. S. S. Brooks, Physica B **172**, 101 (1991); M. S. S. Brooks, O. Eriksson, L. Severin, and B. Johansson, *ibid.* **192**, 39 (1993).

[47]W. Nolting, W. Borgiel, V. Dose, and T. Fauster, Phys. Rev. B **40**, 5015 (1989).